Synthesis, structure and properties of lithium ion conducting lanthanum niobates with defect perovskite structure

Anatolii G. BELOUS[1]*, Oksana N. GAVRILENKO[1], Sofiya D. KOBILYANSKAYA[1], Oleg I. V'YUNOV[1], Volodymyr V. TRACHEVSKII[2], Odile BOHNKE[3]

[1] *V.I.Vernadskii Institute of General and Inorganic Chemistry of the Ukrainian NAS, p. Palladina 32-34, 03680 Kyiv 142, Ukraine.*
[2] *S.V. Kurdyumov Institute of Metal Physics of the Ukrainian NAS, bl. Vernadskoho 36, 03680 Kyiv 142, Ukraine*
[3] *Laboratoire des Oxydes et Fluorures (UMR6010 CNRS), Institut de Recherche en Ingénierie Moléculaire etMatériaux Fonctionnels (FR 2575 CNRS), Université du Maine Av O.Messiaen 72085 Le Mans Cedex9 France*
** Corresponding author. Tel./ fax: 044-424-22-11; e-mail:belous@ionc.kar.net*

Solid solutions with defect perovskite structure have been obtained in the system $Li_{0.5-y}Na_yLa_{0.5}\square Nb_2O_6$ at $0 \le y \le 0.5$. It has been shown that when sodium ions are substituted for lithium ions, an increase in the unit cell volume (*V*) of defect perovskite is observed. The existence of lithium ions with different mobility in the system $Li_{0.5-y}Na_yLa_{0.5}\square Nb_2O_6$ ($0 \le y < 0.5$) has been shown by ^{7}Li NMR. Percolation mechanism of Li ion diffusion in the system $Li_{0.5-y}Na_yLa_{0.5}\square Nb_2O_6$ is not observed. The lithium ion conductivity in $Li_{0.5-y}Na_yLa_{0.5}\square Nb_2O_6$ (at $y \le 0.43$) is higher in comparison with $La_{0.5}Li_{0.5}Nb_2O_6$. This may be due both to the increased amount of more mobile Li^+ ions in sodium-substituted samples and to increase in *V*. Lithium - containing lanthanum niobate $La_{0.5}Li_{0.5}Nb_2O_6$ has been obtained by the Pechini method. It has been shown that the resistance of this sample is lower than that of sample prepared by solid-state reaction method.

Sodium containing lithium - lanthanum niobate/ Lithium ion mobility / Ionic transport / ^{7}Li NMR /Pechini method

Introduction

Lithium ion conducting solid electrolytes are of interest due to the possibility of obtaining on their basis materials with high ionic conductivity for electrochemical devices [1]. Materials based on $Li_{3x}La_{2/3-x}\square_{4/3-2x}Nb_2O_6$ with defect perovskite structure have a considerable number of vacancies and channels for lithium ion migration. This fact allowed us to obtain in $Li_{0.5-y}Na_yLa_{0.5}\square Nb_2O_6$ system materials with high lithium ion conductivity values ($\sigma \sim 10^{-4}$-10^{-5} S cm^{-1} at 290K) [2-6]. When samples are synthesized by the solid-state reaction (SSR) method, coarse-grained powders are formed [4]. It is known from literature that when the particle size of lithium ion conducting electrolyte is reduced, the cycle life of electrochemical power sources increases [7]. Precipitation from solution allows one to synthesize $La_{0.5}Li_{0.5}Nb_2O_6$ with particles of smaller size [8]. However, the product is not homogeneous since it is impossible to obtain insoluble lithium precipitate. At the same time, the Pechini method, which is employed in the synthesis of many functional materials, allows one to obtain nanosized particles and to homogenize the mixture at molecular level [9].

We had shown earlier [3, 5] that one of the main factors that determines ionic conductivity (σ) in $Li_{3x}La_{2/3-x}\square_{4/3-2x}Nb_2O_6$ is a structural factor. In particular, migration of Li ions is limited by the area of the bottleneck formed by four adjacent oxygen octahedra [10] (Fig 1). The size of structural channel is dependent on the radius of the ions of perovskite A-sublattice (Fig 1). Refs [11-14] show that the partial or complete substitution of La^{+3} ions (r_{CN12}=1.32 Å) and Li^+ ions (r_{CN6} = 0.74 Å) in perovskites by ions of larger size, Sr^{+2} (r_{CN12} = 1.44 Å), increases the ionic conductivity of these materials. Interesting results were obtained when substituting Na^+ ions (r_{CN6}=1.02 Å) for Li^+ ions in the system $Li_{3x}La_{2/3-x}\square_{1/3-2x}TiO_3$ [15-16]. At $y > 0.2$, percolation mechanism of lithium conductivity is observed. This manifests itself by rapid decrease in conductivity because of blocking of lithium ion migration paths by Na^+ ions. It has been shown by neutron diffraction study and NMR spectroscopy that Li^+ shifts to the centers of the unit cell faces, whereas Na^+ and La^{+3} ions are located in the center of unit cell [15, 16]. The existence of lithium ions with different mobility has also been shown [17, 18].

In $Li_{3x}La_{2/3-x}\square_{4/3-2x}Nb_2O_6$ system, the number of vacancies is much larger than that in titanates. Extra vacancies exist owing to the presence of planes in the structure which are completely free from La^{+3} ions (Fig 1). This allows one to assume that the mechanism of lithium ion diffusion in niobates differs from that in titanates. In the works [19, 20], an increase in unit cell volume of samples in $La_xLi_{0.5-y}Na_y\square Nb_2O_6$ and in ionic conductivity on increasing the Na^+ content was observed. In these works Na^+ ions were substituted both for Li^+ ions and for La^{+3} ions. In this case, subject to electroneutrality condition, the number of vacant positions ($\square$) decreases. Besides, since the ionic radius

of Na^+ is smaller than that of La^{+3}, the substitution of lanthanum can lead to a decrease in *V* of perovskite. Therefore, the isovalent substitution of Na^+ ions only for Li^+ ions in the system of lithium ion conducting lanthanum niobates is preferable for the preparation of lithium-containing materials.

The aim of this work was to prepare lithium-containing materials of the $Li_{0.5-y}Na_yLa_{0.5}\square Nb_2O_6$ system ($0.0 \le y \le 0.5$) and to investigate their structure and ionic conductivity.

Experimental

$Li_{0.5-y}Na_yLa_{0.5}Nb_2O_6$ samples (y = 0.0, 0.1, 0.2, 0.3, 0.4, 0.43, 0.46, 0.48, 0.5) were synthesized by the solid-state reaction technique (SSR). High-purity La_2O_3, Nb_2O_5, Li_2CO_3, Na_2CO_3 were used as initial reagents. The synthesis procedure is described in detail in [3, 5]. Samples were pressed and calcined at 970 K for 4 hours. After grinding, they were calcined at 1320 K (time 2h). Sintering was carried out at 1470 – 1550 K (time 2h). The density of ceramic was 4.88 – 5.05 g/cm^3.

To determine the effect of synthesis method on the ionic conductivity, $Li_{0.5-y}Na_yLa_{0.5}\square Nb_2O_6$ sample (y = 0) was also synthesized by Pechini method. In Pechini method, crystalline hydrates $LiNO_3 \cdot 3H_2O$, $La(NO_3)_3 \cdot 6H_2O$ and $NbCl_5$ (all chemical-purity grade) were used as initial reagents. Niobium chloride was dissolved in isopropyl alcohol (chemical-purity grade iPrOH). Citric acid (chemical-purity grade CA) and excess ethylene glycol (chemical-purity grade EG) were added to the resulting solution. CA was added to aqueous solutions of $LiNO_3{\cdot}3H_2O$ and $La(NO_3)_3{\cdot}6H_2O$. The solutions were mixed in stiochiometric ratios and heated at 340K under stirring. To obtain xerogel, polymer was calcined additionally at 370 K during 12 h. Precursor powder (LLNbO) was prepared by calcining polymer at 570 K. Ceramic samples were fired in air at 770 - 1520 K during 1 h. The density of ceramic was 4.95 g/cm^3.

The phases were identified by X-ray powder diffraction (XRD) recorded at room temperature with a DRON-4-07 diffractometer (Cu *K*α radiation; 40 kV, 18 mA). Data for sintered samples were collected in the 2θ range from 10 to 150° in a step mode with the step $\Delta 2\theta = 0.02°$ and an exposure time of 6 s for each point. The crystal parameters were refined using Rietveld full-profile analysis.

The electrophysical properties of the ceramic samples were investigated by complex impedance spectroscopy in the frequency range from 1 Hz to 5 MHz using a Solartron 1260 Frequency Gain-Rhase Analyzer coupled with a 1296 Dielectric Interface. Sputtered Pt was used as ion-blocking electrodes. To gain insight into the charge-transport mechanism, electrical conductivity $\boldsymbol{\sigma}$ was measured as a function of temperature and frequency in special cells which enabled $\boldsymbol{\sigma}$ measurements in vacuum, air, and inert atmospheres. Electrical contacts were made by firing silver paste. The specimens were 0.9±0.1 cm in diameter and 0.3±0.2 cm in thickness. The total conductivity was found to be comprised of hole, electronic, and ionic contributions. The electronic conductivity was measured at a dc voltage of 0.5 V, which was low enough to rule out electrolysis. At 570 K, the electronic contribution was no greater than 0.05% of the total conductivity. In evaluating the lithium ion conductivity, we took into account the blocking contacts and interfacial polarization effects

The ^{7}Li NMR spectra have been recorded on an AVANCE 400 spectrometer (Bruker, Germany) at frequencies of 155.51 MHz and 105.84 MHz in a temperature range of 235 - 350 K. The chemical shift of resonating lines is given with respect to $Li(H_2O)_4^+Cl^-$ signals. The profile function parameters of NMR spectra (wide Gaussian and narrow Lorenzian components) were determined using a PeakFit software. The ^{7}Li MAS NMR spectra were registered using the 4 mm ZrO_2 sample rotors and rotation speed 10 kHz.

Results and discussion

System $Li_{0.5-y}Na_yLa_{0.5}\ \ Nb_2O_6$

The XRD results for $Li_{0.5-y}Na_yLa_{0.5}\square Nb_2O_6$ ceramic (Fig. 2) showed formation of single-phase materials with defect-perovskite structure of orthorhombic system (space group Pmmm) in the range $0 \le y \le 0.5$. In the studied range of isovalent substitutions there is a superstructure reflection 101, which indicates additional ordering of structural vacancies [21] in the plane z = ½ (Fig. 1). The intensity of 101 reflection decreases with increasing *y*, which may probably indicate substitution of sodium ions for lithium ions both in the plane *z* = 0 and in the plane *z* = 1/2 , causing structural disordering (Fig. 1, Fig.2).

Table 1 lists structure parameters of $Li_{0.5-y}Na_yLa_{0.5}\square Nb_2O_6$ ceramic. The coordinates in the structure of $Li_{3x}La_{2/3-x}\square_{4/3-2x}Nb_2O_6$ [21] were used as basis approximation. Increase in unit cell volume with increasing *y* takes place in accordance with the Vegart law.

It was shown that large sodium ions cannot participate in ionic transport in $Li_{0.5-y}Na_yLa_{0.5}\square Nb_2O_6$ system [15, 16]. The ionic conductivity is determined by the motion only of Li^+ ions. Fig. 3 (a) shows an Arrhenius plot of the total conductivity (bulk + grain boundary) at different sodium concentration. The conductivity was calculated from impedance data using equivalent electrical model. The concentration dependences of the electrical conductivity and activation energy ($E_{act.}$) of samples $Li_{0.5-y}Na_yLa_{0.5}\square Nb_2O_6$ have been calculated. Isotherms of electrical conductivity against the amount of lithium are shown in Fig. 3 (b). When sodium was substituted for lithium in the system $Li_{0.5-}$

$_{y}Na_{y}La_{0.5}\square Nb_2O_6$, the value of ionic conductivity at 290K increased from $\sigma = 6.85 \cdot 10^{-6}$ S cm^{-1} to $\sigma = 1.28 \cdot 10^{-5}$ S cm^{-1} at $y = 0$ and y = 0.43 respectively. Further increase of y ($y > 0.43$) led to a sharp decrease in σ. In the case when sodium was substituted for lithium, the activation energy of conductivity decreases Fig. 3 (c).

An analysis of the observed dependences (Fig 3 (b-c)) allowed us to conclude that the ionic conductivity of the system $Li_{0.5-y}Na_yLa_{0.5}\square Nb_2O_6$ is affected by two competing factors depending on y. On the one hand, when y is increased, V increases (Table 1), which makes for increase in σ and decrease of $E_{act.}$. On the other hand, increasing the Na^+ concentration leads to a decrease in charge carrier (lithium) concentration and hence to a decrease in conductivity. As a result of the two competing effects, the concentration dependence of the value of lithium ion conductivity has a maximum.

Fig.3 (d) show results of complex impedance of the sample $Li_{0.5-y}Na_yLa_{0.5}\square Nb_2O_6$ in the system at y = 0 ($Li_{0.5}La_{0.5}Nb_2O_6$), obtained by SSR method and Pechini method. We can see that the impedance of sample prepared by Pechini method was smaller than that of sample prepared by solid state reaction technique. It can be explained by the fact that samples synthesized by Pechini method have higher chemical homogeneity, greater density, larger volume of the cell as compared to sample synthesized by SSR (Table 2).

^{7}Li NMR spectra of samples in the system $Li_{0.5-y}Na_yLa_{0.5}\square Nb_2O_6$ as a function of sodium concentration have been obtained (Fig. 4(a-b)). The displacement of NMR in lines (δ) to strong field with increasing the temperature at $y = 0.2$ and $y = 0$ (Fig 4 (a-b)) indicated the action of the resulting field of the ions of the near environment being enhanced (higher degree of screening of lithium nuclei) on increase in σ. The narrowing of lines, which occurs in this case, is connected with increase in ionic conductivity on increasing the temperature. The NMR spectra of all samples under investigation were a superposition of the wide (I_w) and narrow (I_n) components. The presence of two components is accounted for by the presence in the structure of lithium ions which are localized in different planes ($z = 0$, $z = ½$) and have different near environment (Fig. 1) and, obviously, different mobility [16 - 18]. The wide component is responsible for the presence of less mobile lithium ions, whereas the narrow component is responsible for the presence of more mobile lithium ions. The decrease in the ratio I_w / I_n with the substitution of sodium ions for lithium ions (Fig 4 (c)) indicated an increase in the portion of more mobile ions, which may be due to an increase in the unit cell volume of perovskite.

The presence of two types of lithium ions with different mobility is also evidenced by the ^{7}Li NMR spectra of samples of the $Li_{0.5-y}Na_yLa_{0.5}\square Nb_2O_6$ system in the case of sample rotation around a magic angle (Fig. 5). Since ^{7}Li has a nuclear spin $I = 3/2$, the spectra are formed by the central (*-1/2, 1/2*) and two satellite transitions (*1/2, 3/2*) and (*-1/2, -3/2*). These components are modulated by equally spaced bands. The NMR spectra of more mobile lithium ions are formed by the more intense central line, whereas the spectra of less mobile lithium ions are formed by satellite lines. Fig. 5 shown that the intensity of the lines connected with the localized (inside in the cell) motion of lithium ions decreases with increasing y. This indicates an increase in the portion of more mobile lithium ions in sodium-rich samples.

In the system $Li_{0.5-y}Na_yLa_{0.5}\square Nb_2O_6$, as in the system $Li_{0.5-x}Na_xLa_{0.5}TiO_3$ [17, 18], the presence of two types of lithium ions with different mobility is observed. However, a considerable difference between titanates and niobates is noteworthy. The isovalent substitution of sodium ions for lithium ions in $Li_{0.5}La_{0.5}TiO_3$ causes blocking of lithium ion migration channels above a certain Na^+ concentration and percolation mechanism of lithium ion diffusion in this system [15-18]. In the $Li_{0.5-y}Na_yLa_{0.5}\square Nb_2O_6$ system, solid solutions with perovskite structure are formed in the whole concentration range, and an increase in ionic conductivity in comparison with $Li_{0.5}La_{0.5}Nb_2O_6$ is observed. This difference occurs due to some causes. Firstly, the much larger number of vacancies in niobates in comparison with titanates. Secondly, the increase in the size of migration channels with sodium content. It contributes to decrease in the activation energy of ionic conductivity in the system $Li_{0.5-y}Na_yLa_{0.5}\square Nb_2O_6$.

The question of distribution of lithium ions with different mobility over crystallographic position and the diffusion in $Li_{0.5-y}Na_yLa_{0.5}\square Nb_2O_6$ calls for more detailed study.

Conclusions

The formation of solid solutions with defect-perovskite structure in the system $Li_{0.5-y}Na_yLa_{0.5}\square Nb_2O_6$ at $0.0 \le y \le 0.5$ has been established, and their structure peculiarities have been studied. It has been shown that when sodium ions are substitute for lithium ions, an increase in the unit cell volume (V) of defect perovskite is observed. The ionic conductivity passes through a maximum as a result of two competing factors: increase in the unit cell volume of perovskite and decrease in lithium ion concentration. The existence of lithium ions with different mobility in the $Li_{0.5-y}Na_yLa_{0.5}\square Nb_2O_6$ system ($0 \le y < 0.5$) and their role in the ionic transport has been shown by NMR method. Lithium-containing lanthanum niobate $Li_{0.5-y}Na_yLa_{0.5}\square Nb_2O_6$ at $y = 0$ has been obtained by the Pechini method. It has been shown that the resistance of this sample is less than that of sample prepared by solid-state reaction technique.

References

[1] Ye.I. Burmakin, Solid electrolytes with alkali metal ion conductivity (in Russian), Nauka, Moskow (1992) 263.
[2] A. Belous, I. Didukh, E. Novosadova, Y. Pashkova, *Fiz. Tverd. Tela*. 28 (1986) 3230-3232.
[3] A.G. Belous, O.N. Gavrilenko, E.V. Pashkova, V.N. Mirnyi, *Elektrokhimiya* 38 (2002) 479-484.
[4] O.N. Gavrilenko, E.V. Pashkova, B.S. Khomenko, A.G. Belous, *Ukr. Knim. Zh.* 69 (2003) 67-71.
[5] A. Belous, E. Pashkova, O. Gavrilenko, O. V'yunov, L. Kovalenko, *J. Eur. Ceram. Soc*. 24 (2004) 1301-1304.
[6] A.G. Belous, O.N. Gavrilenko, E.V. Pashkova, K.P. Danil'chenko, O.I. V'yunov, *Neorg. Mater*. 40 (2004) 993-1000.
[7] J. Jamnikab, J. Maier, *Phys. Chem. Chem. Phys*. 5 (2003) 5215-5220.
[8] A. Belous, O. Gavrilenko, O. Pashkova, O. Bohnké, C. Bohnké, *Eur. J. Inorg. Chem*. (2008) 4792-4796.
[9] M.P. Pechini, Method of preparing lead and alkaline earth titanates and niobates and coating method using the same to form a capacitor, U.S. Patent, July, 1967.
[10] M.A. Paris, J. Sanz, C. Leon, J. Ibarra, A. Varez, *Chem. Mater*. 12 (2000) 1694-1701.
[11] M. Itoh, Y. Inaguma, W. Jung, L. Chen, T. Nakamura, *Solis State Ionics* 70/71 (1995) 203-207.
[12] V.I. Thangadura, A.K. Shukla, J. Gopalakrishnn, *Chem. Mater.* 11 (1999) 835-839.
[13] H. Watanabe, J. Kuwano, *J. Power Sources*. 68 (1997) 421-426.
[14] O.N. Gavrilenko, A.G. Belous, L.L. Kovalenko, Ye.V. Pashkova, *Materials and Manufacturing Processes* 23 (2008) 607-610.
[15] A. Rivera, C. León, J. Santamaría, A. Várez, O. V'yunov, A. Belous, J. Alonso, J. Sanz, *Chem. Mater*. 14 (2002) 5148-5152.
[16] M. Sanjuan, M. Laguna, A. Belous, O. V'yunov, *Chem. Mater*. 17 (2005) 5862-5866.
[17] O. Bohnke, *Solid State Ionics* 179 (2008) 9-15.
[18] R. Jimene, A. Rivera, A. Varez, *J.* Sanz, *Solid State Ionics* 180 (2009) 1362-1371.
[19] T. Katsumata, Y. Inaguma, M. Itoh, *Solid State Ionics*. 113-115 (1998) 465-469.
[20] Y. Jin Shan, N. Sinozaki, T. Nakamura, *Solid State Ionics*. 108 (1998) 403-406.
[21] V. B. Nalbandyan, I. A. Shukaev, *Zh. Neorg. Khim*. 34 (1989) 793-795.

Table 1 Structure parameters of complex oxides in the system $Li_{0.5-y}Na_yLa_{0.5}\square Nb_2O_6$ as a function of sodium content (y).

y	0.1	0.2	0.3	0.4	0.43	0.46	0.48	0.5
Unit cell parameters								
a, Å	3.903(8)	3.906(8)	3.915(1)	3.915(9)	3.923(1)	3.918(1)	3.9167(8)	3.925(1)
b, Å	3.904(7)	3.907(8)	3.912(1)	3.915(9)	3.9311(6)	3.923(1)	3.9304(7)	3.9278(6)
c, Å	7.854(2)	7.852(1)	7.861(1)	7.861(1)	7.850(2)	7.860(2)	7.846(2)	7.848(3)
V, $Å^3$	119.7(3)	119.8(4)	120.40(5)	120.5(2)	121.07(5)	120.79(6)	120.78(4)	120.98(6)
Coordinates of ions								
Nb, z/c	0.254(2)	0.256(1)	0.256(1)	0.259(1)	0.2527(8)	0.2551(9)	0.2582(9)	0.251(1)
O3, z/c	0.24(2)	0.30(4)	0.26(2)	0.3(3)	0.28(1)	0.26(4)	0.260(6)	0.29(4)
O4, z/c	0.21(2)	0.28(4)	0.29(2)	0.3(3)	0.29(1)	0.26(4)	0.272(7)	0.28(4)
Agreement factors								
R_f, %	6.42	6.98	5.92	5.36	7.36	6.30	5.94	6.40
R_{exp},%	8.62	9.15	9.78	8.36	5.01	4.84	4.18	8.96

Table 2 Structure parameters of $Li_{0.5}La_{0.5}Nb_2O_6$ samples, obtained by two synthesis methods.

Method of synthesis	SSR	Pechini method
Unit cell parameters		
a	3.9002(1)	3.903(1)
b	3.9005(1)	3.908(1)
c	7.8521(2)	7.868(6)
V, A^3	119.4521(6)	120.01(6)
Coordinates of ions		
Nb, z/c	0.2580(2)	0.259(1)
O3(O4), z/c	0.23(1)	0.230(6)
Agreement factors		
R_B, %	8.5	8.10
R_f, %	9.2	9.19

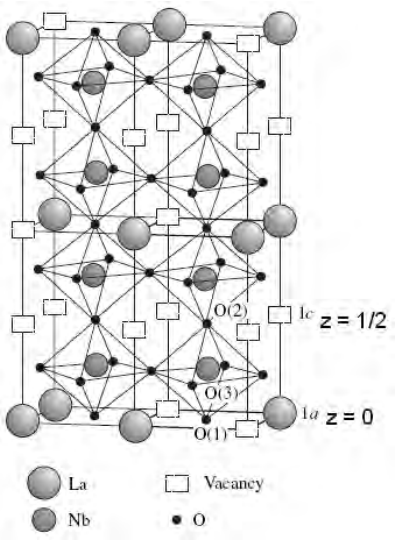

Fig. 1 Structure of the A-site deficient perovskite $La_{2/3\ \ 4/3}Nb_2O_6$ (sp. gr. Pmmm): La in position 1a (000), Nb in 2t (1/2 1/2 z), O(1) in 1f (1/2 1/2 0), O(2) in 1h (1/2 1/2 1/2), O(3) in 2s (1/2 0 z), O(4) in 2r (0 1/2 z), and vacancies in 1c (0 0 1/2).

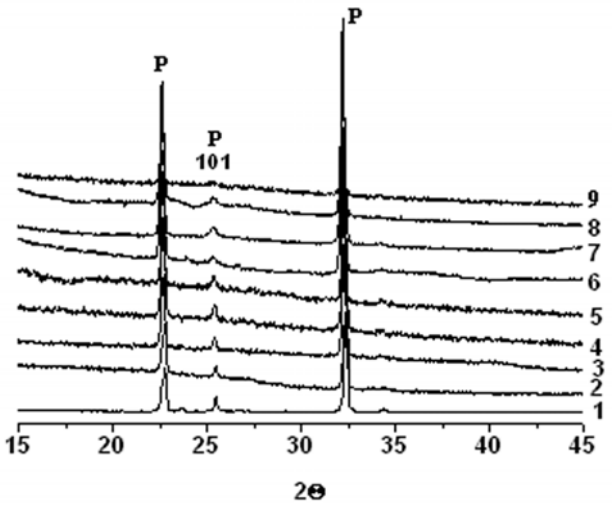

Fig. 2 X-ray diffraction patterns of sintered $Li_{0.5-y}Na_yLa_{0.5}\square Nb_2O_6$ samples at different sodium concentrations: 1 - y = 0; 2 - *y* = 0.1; 3 - *y* = 0.2; 4 - *y* = 0.3; 5 - *y* = 0.4; 6 - *y* = 0.43; 7 - *y* = 0.46; 8 - *y* = 0.48; 9 – *y* = 0.5.

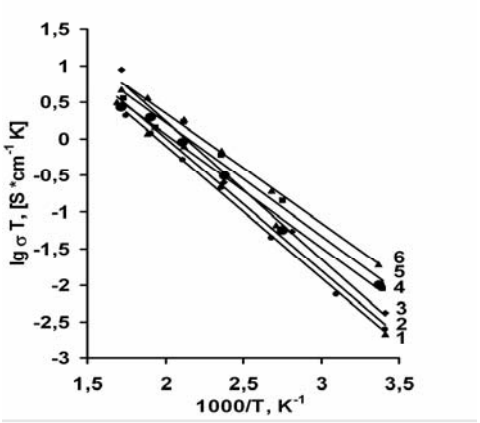

a

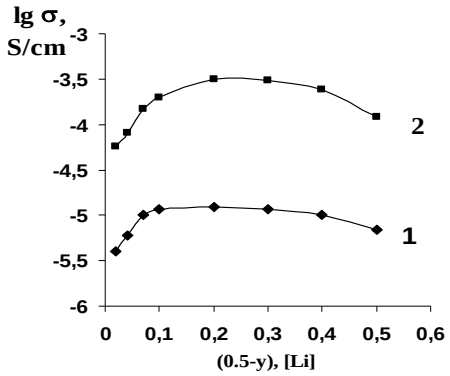

b

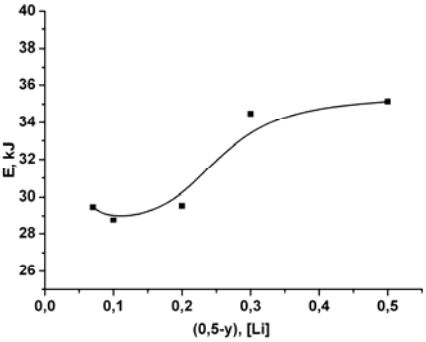

c

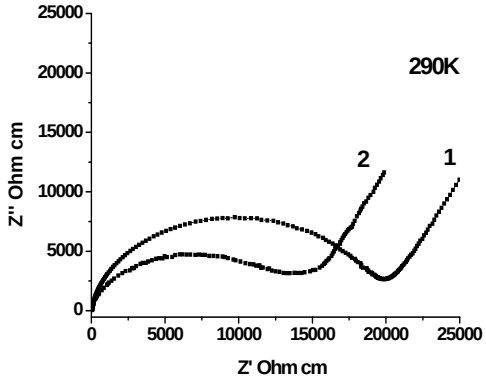

d

Fig. 3 Electrophysical properties of the system $Li_{0.5-y}Na_yLa_{0.5}\square Nb_2O_6$

(a) Arrhenius plots of the total ionic conductivity of sintered pellets of $Li_{0.5-y}Na_yLa_{0.5}\square Nb_2O_6$ at various sodium concentrations: 1 - y = 0; 2 - y = 0.2; 3 - y = 0.3; 4 - y = 0.4; 5 - y = 0.43; 6 - y = 0.46.

(b) Isotherms of ionic electrical conductivity as a function of lithium concentration [Li] in the system $Li_{0.5-y}Na_yLa_{0.5}\square Nb_2O_6$ at various temperatures: 1 – 290K; 2 – 370K.

(c) Activation energy of conductivity (E_a) of $Li_{0.5-y}Na_yLa_{0.5}\square Nb_2O_6$ as a function of lithium content [Li]

(d) Plots of complex impedance of the sample $Li_{0.5-y}Na_yLa_{0.5}\square Nb_2O_6$ (y = 0) prepared by SSR method (1) and Pechini method (2). T = 290K

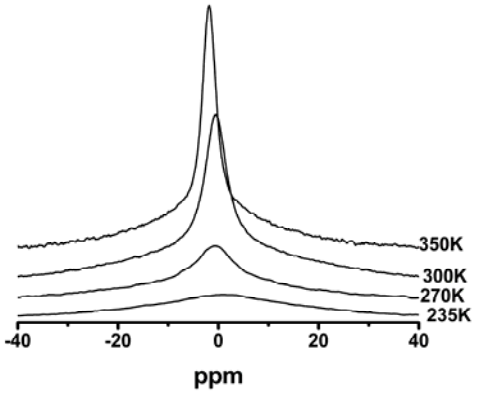

a

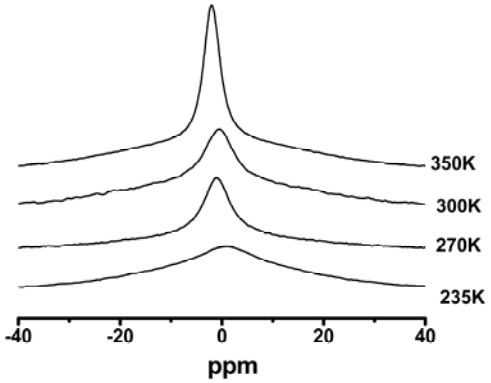

b

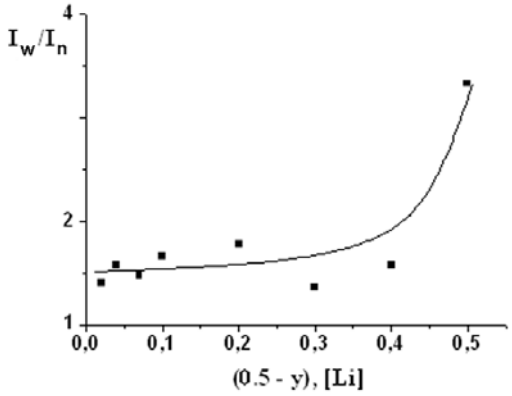

Fig. 4 ^{7}Li NMR spectra of the system $Li_{0.5-y}Na_yLa_{0.5}Nb_2O_6$

(a) $y = 0.2$;

(b) $y = 0$;

(c) ratio of intensity of the wide and narrow components (I_w/I_n) of ^{7}Li NMR spectrum T = 290 K.

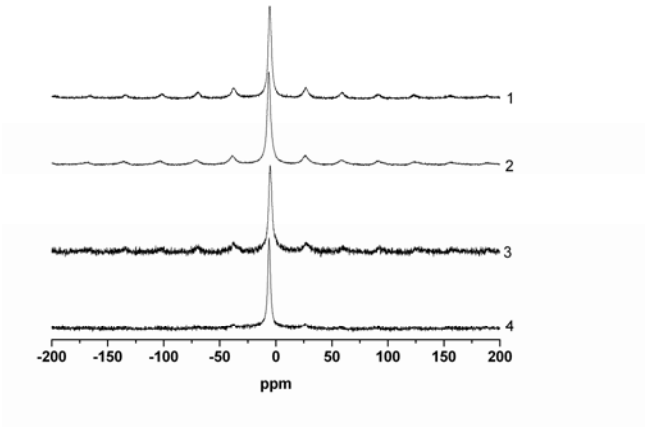

Fig. 5 ^{7}Li MAS - NMR spectra of $Li_{0.5-y}Na_yLa_{0.5}Nb_2O_{6,}$ at various sodium concentrations: 1 - y = 0; 2 - y = 0.4; 3 - y = 0.43; 4 - y = 0.48. T = 290 K